

32. MAGNETOSTRATIGRAPHY OF SITES 782, 783, 784, AND 786, IZU-BONIN OUTER FOREARC, WESTERN PACIFIC¹

J. R. Ali,² R. B. Haston,³ and L. B. Stokking⁴

ABSTRACT

During Leg 125, scientists drilled Sites 782, 783, 784, and 786 across a transect of the Izu-Bonin forearc near 31°N. Magnetostratigraphy for whole-core and discrete specimens has been integrated with biostratigraphic data and correlated to the geomagnetic polarity time scale. These correlations are good back to the middle Miocene at Sites 783, 784, and 786 and to the late Oligocene at Site 782, but become more tentative in older sediments because of poor recovery and complex magnetizations.

INTRODUCTION

Ocean Drilling Program (ODP) Sites 782, 783, 784, and 786 form a transect close to 31°N across the outer part of the Izu-Bonin forearc. Paleomagnetic, biostratigraphic, and sedimentological data provide scientists an opportunity to investigate the evolution of this forearc terrain, where the Pacific plate has been subducting beneath the Philippine Sea plate since the Eocene. The paleomagnetic record obtained from the forearc sequences recovered at these sites is generally good from the middle/late Miocene to the present. Earlier than that, a combination of low sediment accumulation, sedimentary hiatuses, unstable magnetizations, and poorer biostratigraphic data (because of calcite dissolution) makes correlation with the standard geomagnetic polarity time scale (GPTS) of Berggren et al. (1985) less reliable. However, several well-defined magnetostratigraphic boundaries that have been correlated with this scale permit one to calculate sedimentation rates in the Izu-Bonin forearc. Future work with these data will help develop a depositional history for the area that can be used to unravel the enigmatic tectonic history of the Izu-Bonin forearc.

LITHOLOGIC UNITS

Hole 782A (Fig. 1) was drilled on the eastern margin of the Izu-Bonin forearc basin, about halfway between the active volcanic arc and the trench. Two lithologic units were identified in this hole. Unit I (0–409.2 m below seafloor, or mbsf) comprises a sedimentary succession from Pleistocene to late Eocene in age and is divided into three subunits (Subunit IA, 0–153.6 mbsf; Subunit IB, 153.6–337.0 mbsf; and Subunit IC, 337.0–409.2 mbsf). This unit consists primarily of nannofossil-rich marls and some chalks, together with abundant volcanic debris. Recovery through Unit I averaged just under 70%. Two unconformities have been identified in the sediments: one between upper Oligocene and lower Miocene sediments and another between upper Eocene and lower Oligocene sediments. Unit II (409.2–476.8 mbsf), recovered as gravel-sized chips, comprises intermediate-acid volcanic rocks that form basement.

Site 783 (Fig. 1) is located on the northern mid-flank portion of the Torishima forearc serpentinite seamount, on the inner wall of the Izu-Bonin trench. Two lithologic units were identified in the single hole drilled at this site. Unit I (0–120.0 mbsf) comprises a mid-Pleis-

tocene to lower Pliocene, or older, sequence of glass-rich clay and claystone. Unit II (120.0–158.6 mbsf) is a phacoidal sheared serpentinite (Fryer, Pearce, Stokking, et al., 1990) that contains clasts of harzburgite, but was not sampled for this study.

Hole 784A (Fig. 1) is located on the western flank of the same seamount. Two lithologic units were identified in this hole. Unit I is subdivided into Subunits IA (0–126.4 mbsf), IB (126.4–302.7 mbsf), and IC (302.7–321.1 mbsf). It consists primarily of clays and claystone together with a significant vitric component. Subunit IC also contains a notable amount of clay and silt-sized serpentinite. Unit II (321.1–425.3 mbsf) is a phacoidal sheared serpentinite microbreccia.

Site 786 (Fig. 1) is located in the center of the Izu-Bonin forearc basin, about 200 km east of the active volcano Myojin Sho. Three sedimentary units were identified in Hole 786A. Unit I (0–83.46 mbsf) consists of lower Pleistocene to middle Miocene nannofossil marls and clays. Unit II (83.46–103.25 mbsf) comprises a sequence of upper Oligocene to middle Eocene nannofossil marls and nannofossil-rich clays with abundant volcaniclastic debris. Unit III (103.25–124.90 mbsf) is a series of volcaniclastic breccias. Unit IV (Hole 786A: 124.9–166.5 mbsf; Hole 786B: 162.5–826.6 mbsf) is a volcanic sequence that forms basement.

METHODS

Paleomagnetic measurements of sediments from the Izu-Bonin forearc were performed using (1) the shipboard three-axis whole-core 2G-cryogenic (WCC) magnetometer and (2) the discrete-specimen fluxgate (DSF) magnetometer (manufactured by Molspin) in the Southampton University paleomagnetic laboratory. The WCC magnetometer was used to measure paleomagnetism at 10-cm intervals along the length of all archive-half cores, whereas the DSF was used for discrete specimens contained in standard 7-cm³ ODP paleomagnetic sample cubes. Typically, one discrete specimen was taken from each 1.5-m section of core. Alternating field (AF) demagnetization was used to remove low-stability (low-coercivity) components of magnetization. The WCC system has a three-axis AF demagnetizer mounted in line with the magnetometer, and the archive-half cores were demagnetized to a maximum field of 10 mT. The discrete specimens were demagnetized using a Molspin rotating specimen system to maximum fields of 40 to 50 mT. The cores are unoriented-polarity is assessed on the basis of inclination only.

At Site 782, a total of 179 specimens was taken from Unit I for this study. The gravel-sized chips of Unit II were too broken-up for paleomagnetic work. Twenty-five specimens were taken from the upper 66.01 m of Unit I at Site 783. In the lower half of the unit, the core recovery was low, and the material retrieved was too disturbed for paleomagnetic work. No samples were taken for this investigation from the sheared phacoidal serpentinite of Unit II. A total of 126 paleomagnetic specimens was taken from Unit I at Site 784; no

¹ Fryer, P., Pearce, J. A., Stokking, L. B., et al., 1992. *Proc. ODP, Sci. Results*, 125: College Station, TX (Ocean Drilling Program).

² Department of Oceanography, University of Southampton, SO9 5NH, United Kingdom.

³ Department of Geological Sciences, University of California, Santa Barbara, CA 93106, U.S.A. (Present address: AMOCO Production Company, 501 West Lake Park Boulevard, P.O. Box 3092, Houston, TX 77253, U.S.A.)

⁴ Ocean Drilling Program, Texas A&M University, 1000 Discovery Drive, College Station, TX 77845-9547, U.S.A.

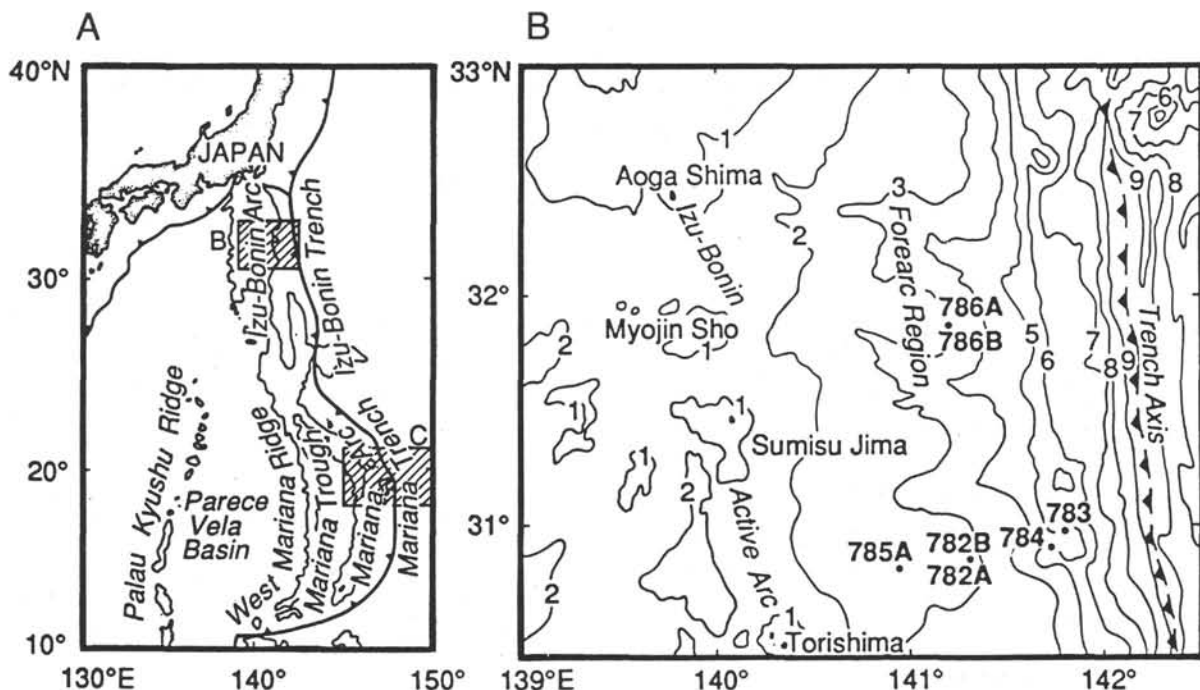


Figure 1. Location of Sites 782, 783, 784, and 786 in the Izu-Bonin forearc.

samples were analyzed from Unit II, a sheared phacoidal serpentine microbreccia. Thirty discrete samples were taken from Unit I at Site 786 for this study. Although paleomagnetic specimens were taken from Unit IV at Site 786, a volcanic basement sequence, none of the data is presented in this paper.

AF DEMAGNETIZATION AND MAGNETIC STABILITY

All archive-half cores, except those showing noticeable drilling disturbance, were processed using the WCC. Measurements of the natural remanent magnetization (NRM) and the remanence remaining after demagnetization to 10 mT were conducted on the cores; the intensity typically decreased to about 20% to 40% of NRM after demagnetization at 10 mT. Changes in both the remanence declination and inclination of up to a few tens of degrees are typical (see Appendix A).

As nearly all of the discrete specimens had NRM intensities of >20 mA/m, these were processed using the DSF (noise level = <0.05 mA/m), together with a Molspin tumbler, for demagnetization to 40 to 50 mT. Unfortunately, a small number of the specimens from Holes 782A (7%) and 784A (4%) and a significant proportion from Hole 786A (41%) proved too unstable to measure beyond values of about 15 mT, and these data should be ignored. Note that all these specimens are from intervals where the sedimentation rate is a few meters per million years (Fryer, Pearce, Stokking, et al., 1990).

Typical examples of demagnetization data from the discrete specimens are shown in Figure 2. In all cases, small to moderate changes in the direction of remanent magnetism occur during demagnetization of up to 5 to 10 mT, but thereafter the trajectories are generally directed toward the origin.

MAGNETIC POLARITIES AND STRATIGRAPHIC CORRELATIONS

The magnetic polarity history for each hole is based on both the WCC data (Appendix A) and DSF data (Appendix B). These data

have been used to define a polarity log (Figs. 3 through 6) for each of the holes, and the DSF data have been used to verify the much higher resolution WCC magnetostratigraphy. The WCC records include a number of magnetozones (up to a few tens of meters) that contain short (a few tens of centimeters) intervals of opposite polarity. Discrete-specimen data from a number of these levels confirm these short-term polarity inversions within the WCC record.

Biostratigraphic control is provided by calcareous nannofossils (Ciampo, this volume; Xu and Wise, this volume) and diatoms (Stabell, this volume). The sequences of magnetic polarity zones identified in each of the holes are matched with the GPTS of Berggren et al. (1985).

Hole 782A

The magnetostratigraphic record for Hole 782A (Fig. 3) is reliable between 0 and 322 mbsf, where there is close agreement between the WCC and DSF data. Below this level, the DSF data are in many cases of opposite polarity to the equivalent level in the WCC record, indicating that 10-mT demagnetization was insufficient to remove the effects of secondary magnetizations. In the lower part of this hole, the WCC record is dominated by thinner magnetozones. However, the biostratigraphic data at these levels indicate sedimentation rates that average about 1 to 3 m/m.y., and these therefore may represent a condensed magnetostratigraphic record. As insufficient DSF data exist from these levels to confirm the WCC results, one should not place too much emphasis on the WCC data.

The start of the normal polarity Brunhes Chron is positioned at 24.8 mbsf. The reverse polarity Matuyama Chron begins at 66.20 mbsf and includes records of the Jaramillo (29.1–34.6 mbsf) and Olduvai (47.8–53.5 mbsf) normal polarity subchrons. Incomplete recovery and poor biostratigraphic control prevented us from locating the normal polarity Gauss Chron precisely, but normal polarity intervals corresponding to this chron have been recorded in Cores 125-782A-8H to 125-782A-12X (66.8–115.0 mbsf). All these cores have been assigned to nannofossil Zone CN12. Portions of the reversed

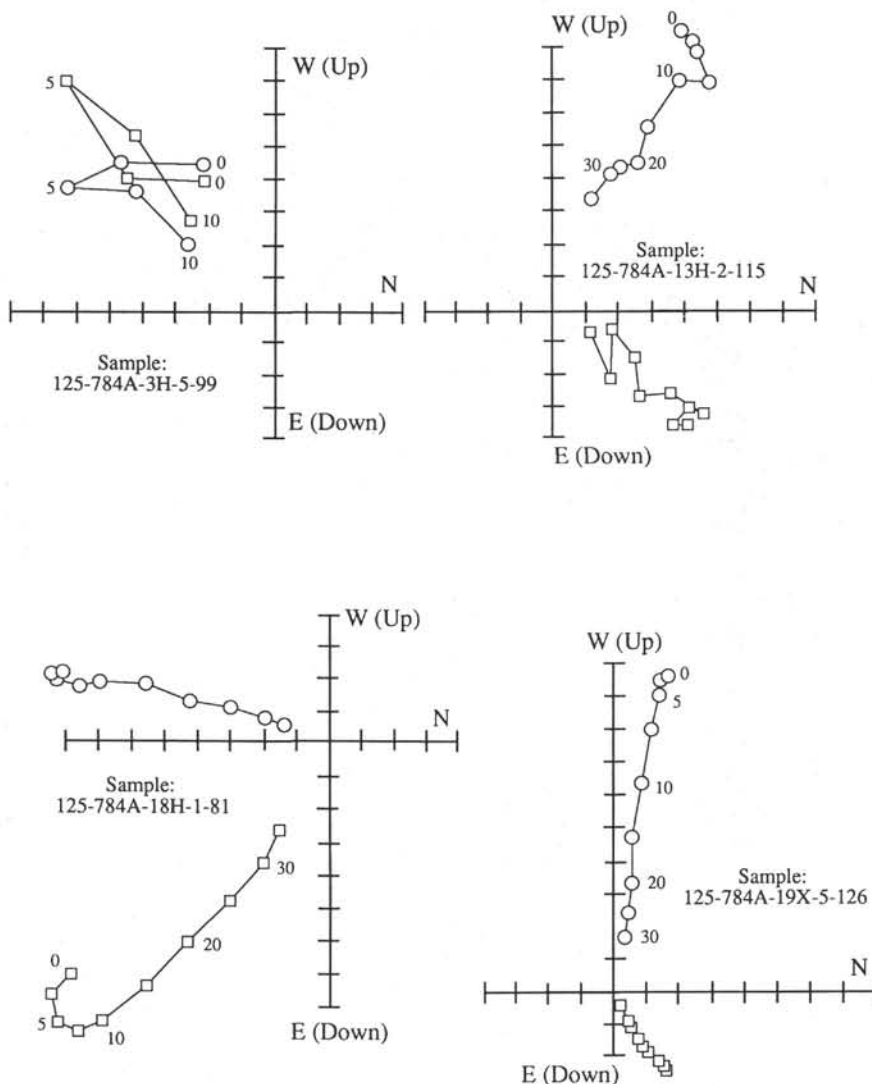


Figure 2. Vector end-point diagrams showing the AF demagnetization behavior of typical discrete specimens from Hole 784A. Demagnetization data are for 5, 10, 15 or 20, 30, and 40 mT. "N," "E," "S," and "W" refer to an arbitrary reference azimuth because the specimens are from unoriented cores. Intensities have been normalized to natural remanent magnetization values. Circles represent projection onto the vertical plane; squares represent projection onto the horizontal plane.

polarity Gilbert Chron were identified within Cores 125-782A-13X to 125-782A-16X (117.7 to 160.2 mbsf) and include partial records of the Cochiti, Nunivak, and Thvera normal polarity subchrons.

Between 160.2 and 245.5 mbsf, the cores have been assigned to nannofossil Zone CN9 and the lower half of Zone 10A. Assuming a constant sedimentation rate (about 25 m/m.y.) throughout this part of the succession, the hole probably contains partial records of Chron 5 through to Chron 9.

Cores 125-782A-26X and 125-782A-27X (240.3–259.6 mbsf) exhibit predominantly normal polarity. The nannofossil Zones CN6 (248.6–253.7 mbsf) and CN7 (245.5–248.6 mbsf) are succeeded by Zone CN9 (the base of which is defined at 245.5 mbsf). Chron C5 is associated with Zones CN6 and CN7, and a correlation of the interval from 245.5 to 253.7 mbsf with this chron is proposed. The base of Zone CN9 is within the same block of normal polarity; thus the normal polarity sediments above 245.7 mbsf must correlate with parts of Chron 9. The hiatus inferred by the absence of nannofossil Zone CN8 from the succession is supported by the apparently discontinuous

paleomagnetic record and by the lack of reversed polarity sediments that would correlate with the early part of Chron 9 and with Chron 10.

Cores 125-782A-28X to 125-782A-34X (259.6–322.5 mbsf) contain nannofossil Zone CN5(a/b), which spans 3.6 m.y. One can correlate the normal polarity intervals within this sequence to Chrons C5A (261.8–267.25 mbsf), C5AAN (278.8–282.1 mbsf), C5ABN (289.35–282.1 mbsf), C5ACN (297.55–300.1 mbsf), and C5AD (303.5–308.7 mbsf).

Correlation below this level is more tentative. Chrons C8, C9, and C10 (within the late Oligocene nannofossil Zone CP19) may occupy parts of the interval between 332.1 and 351.0 mbsf, below which correlation is impossible.

Hole 783A

Only the sediments from the upper half of Unit I in Hole 783A were suitable for paleomagnetic studies. The polarity record (Fig. 4) contains two normal polarity magnetozones (identified in Cores

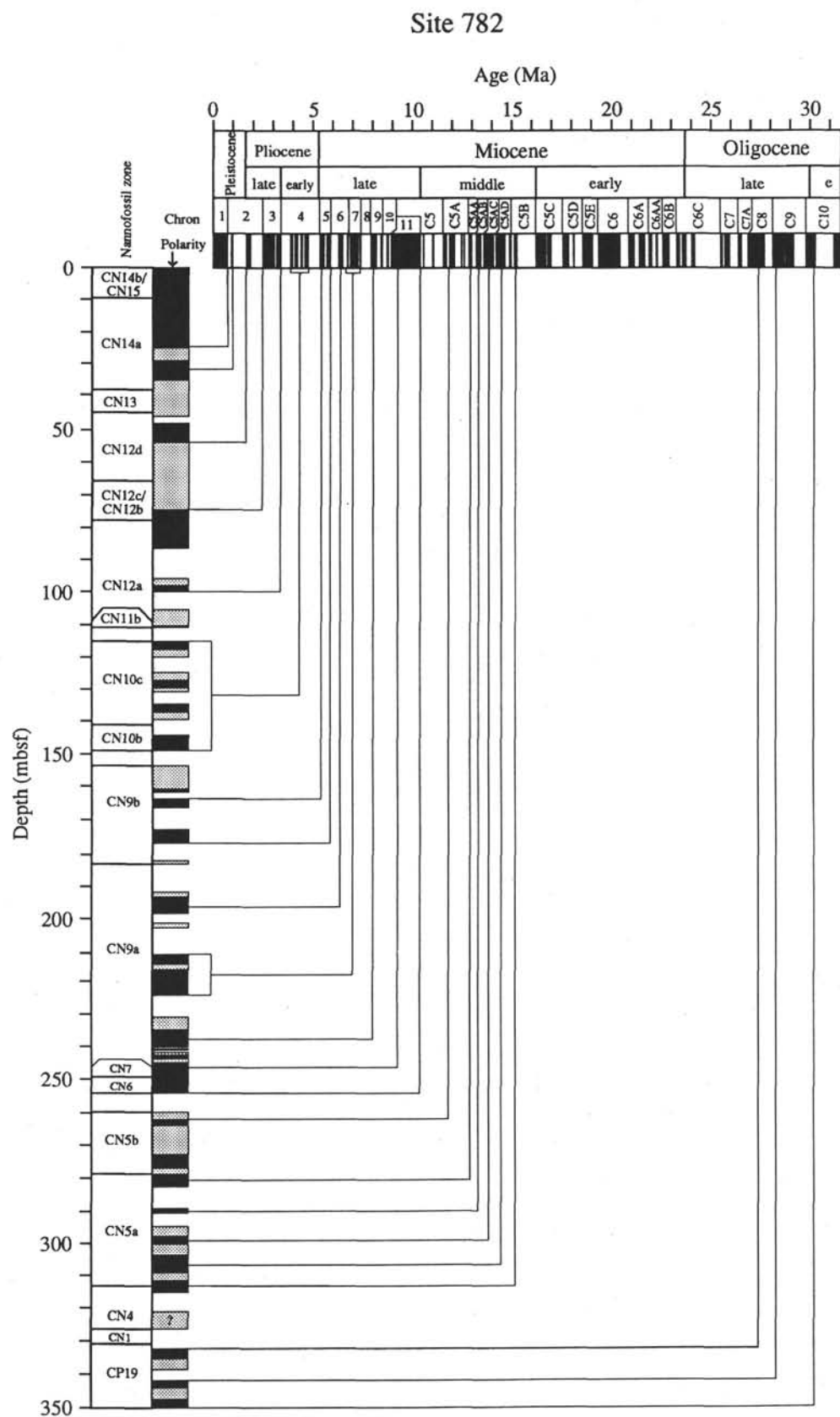


Figure 3. Correlation of the magnetic polarity record for Hole 782A (to 350 mbsf) with the GPTS of Berggren et al. (1985). Black indicates normal polarity, the stippled pattern represents reversed polarity, and blank areas indicate regions of no recovery or no data.

Site 783

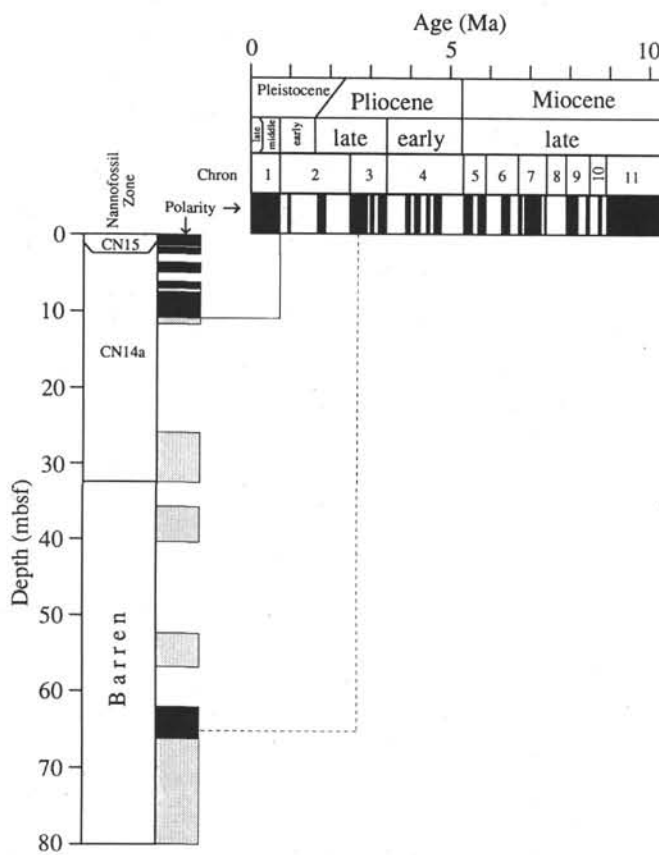


Figure 4. Correlation of the magnetic polarity record for Hole 783A (to 80 mbsf) with the GPTS of Berggren et al. (1985) via the scale of Barron (1985). Black indicates normal polarity, the stippled pattern represents reversed polarity, and blank areas indicate regions of no recovery or no data. The broken line indicates that the correlation is tentative.

125-783A-1R, 0–9.7 mbsf, and 125-783A-8R, 62.1–71.8 mbsf) separated by an interval of reversed polarity. Unfortunately, no polarity transitions have been identified within any of the cores.

Biostratigraphic data for Hole 783A are based primarily on diatoms; because of calcite dissolution only two calcareous nannofossil datums have been identified. Correlations with the GPTS are via the scale proposed by Barron (1985). Core 125-783-1R (0–9.7 mbsf) contains the diatom Zones *Nitzschia reinholdii* and *Pseudoeunotia doliolus*, which indicates an early/middle Pleistocene age. The normal polarity magnetization within this core is a record of the Brunhes Chron. Cores 125-783A-2R (9.7–16.4 mbsf), 125-783A-4R (26.0–35.7 mbsf), 125-783A-5R (35.7–42.7 mbsf), and 125-783A-7R (52.4–62.1 mbsf) contain faunal assemblages that correlate with the nannofossil CN14A Zone and diatom *Rhizosolenia praebergonii* Zone; thus, these cores are early Pliocene to middle Pleistocene in age. The reversed polarity magnetization within these four cores records the Matuyama Chron. Unfortunately, core recovery at these levels averaged 35%, and none of the normal polarity subchrons within the Matuyama Chron have been identified. The normal polarity Gauss Chron is represented in Core 125-783A-8R (62.1–71.8 mbsf).

Hole 784A

Although the sedimentary sequence in Hole 784A extends to 321.1 mbsf, below about 190 mbsf (Core 127-784A-21R) structural com-

Site 784

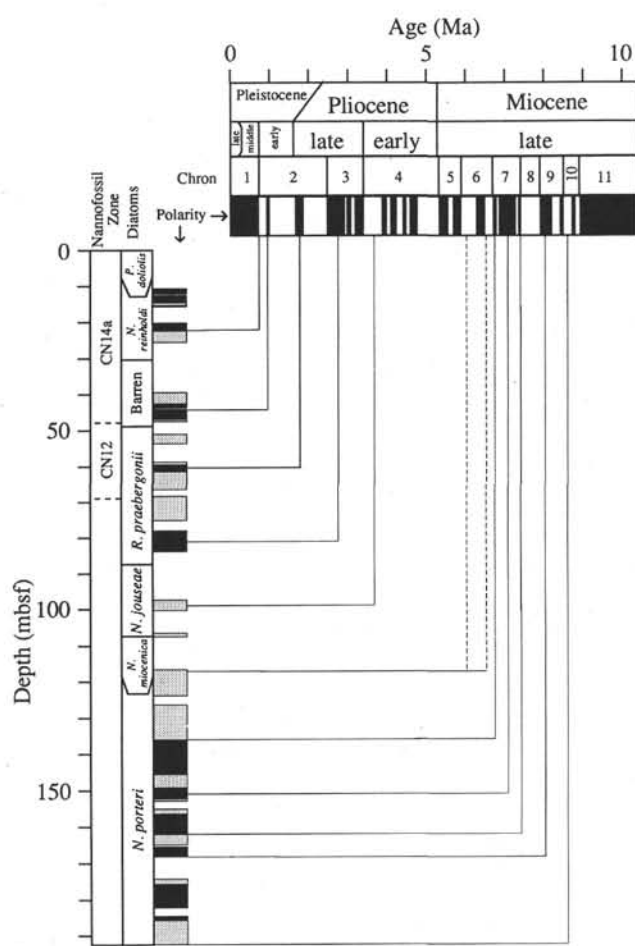


Figure 5. Correlation of the magnetic polarity record for Hole 784A (to 190 mbsf) with the GPTS of Berggren et al. (1985) via the scale of Barron (1985). Black indicates normal polarity, the stippled pattern represents reversed polarity, and blank areas indicate regions of no recovery or no data. Correlations indicated by broken lines are more tentative than those indicated by solid lines.

plications that include shear zones, normal and reverse faults, and bedding dips ranging from 35° to 70° (Fryer, Pearce, Stokking, et al., 1990, pp. 285–289) make correlation with the GPTS unreliable. Biostratigraphic information from the recovered sediments is limited to a sparse diatom assemblage and two calcareous nannofossil events; core recovery averaged only 56.6%. We present tentative correlations from the upper part of the hole (Fig. 5).

The start of the normal polarity Brunhes Chron was recorded at 22.4 mbsf (within Core 125-784A-4R, 20.4–29.9 mbsf). The Jaramillo and Olduvai normal polarity subchrons, within the reversed polarity Matuyama Chron, are positioned between 42.75 and 47.0 mbsf and 59.5 and 61.6 mbsf, respectively. A partial record of the normal polarity Gauss Chron was identified between 78.1 and 83.9 mbsf; this probably represents the youngest normal polarity interval assigned to this chron. A small portion of the reversed polarity Gilbert Chron probably is represented between 97.4 to 100.2 mbsf, as this interval was assigned to the *Nitzschia jouseae* diatom zone.

Sediments in Cores 125-784A-14R and 125-784A-15R (116.7 to 136.0 mbsf) are assigned to the *N. jouseae* and *Nitzschia porteri* diatom zones. Thus, intervals of reversed polarity within these cores

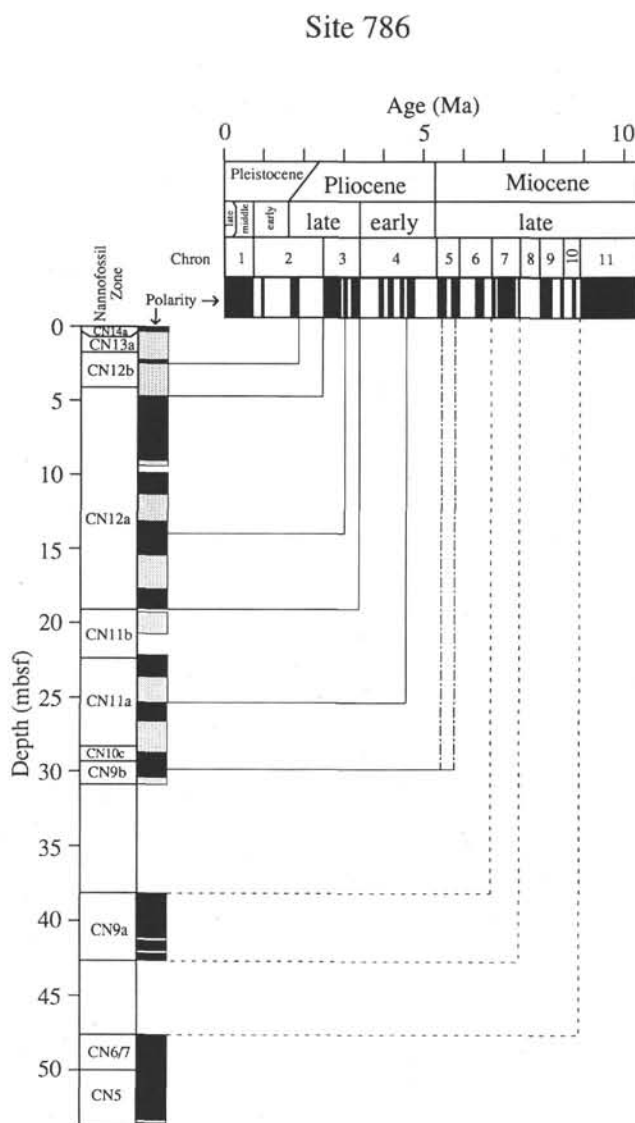


Figure 6. Correlation of the magnetic polarity record for Hole 786A (to 55 mbsf) with the GPTS of Berggren et al. (1985). Black indicates normal polarity, the stippled pattern represents reversed polarity, and blank areas indicate regions of no recovery or no data. Correlations indicated by broken lines are more tentative than those indicated by solid lines. The dashed-and-dotted lines indicate two possible correlations.

probably represent portions of Chron 5 and the later part of Chron 6. No record was found of the *Thalassiosira convexa* Zone that Barron (1985) observed between these two zones.

Cores 125-784A-16R to 125-784A-20R (136.00–182.1 mbsf) were assigned to the *N. porteri* Zone. The polarity sequence recorded by these cores may represent portions of Chrons 6 (lower part) and 7. The identification of the *Coscinodiscus yabei* Zone, identified in Core 125-784A-21R (184.4–194.0 mbsf), reinforces this correlation.

Hole 786A

Interpretation of the WCC and DSF data (Fig. 6) has been restricted to the upper six cores (53.95 mbsf). From this level to Core 125-786A-11X (96.0–105.7 mbsf), the DSF specimens exhibit complex magnetic behavior; obtaining reliable data from these levels proved impossible. Cores 125-786A-1H to 125-786A-6X (0–57.1 mbsf) range in age from early/middle Pleistocene (Zone CN14) to middle Miocene (CN5 at 53.95 mbsf).

The reversed polarity Matuyama Chron has been interpreted as beginning at 4.65 mbsf; the interval between 2.2 and 2.5 mbsf may record the Olduvai normal polarity subchron. The interval from 4.65 to 19.15 mbsf was assigned to the nannofossil Zone CN12a, and thus may represent the Gauss Chron.

The polarity sequence observed between 28.7 and 30.4 mbsf suggests that this interval may contain a partial record of Chron 5. The interval from 38.2 to 42.65 mbsf contains nannofossils from Zone CN9a, which correlates with Chron 7. Chron C5N was partially recorded between 47.6 and 53.95 mbsf, based on the presence of nannofossils from the upper part of Zone CN5 and from Zone CN6/7.

CONCLUSIONS

During Leg 125, Sites 782, 783, 784, and 786 were drilled across a transect of the Izu-Bonin forearc near 31°N that yielded sedimentary sequences suitable for magnetostratigraphic analysis. Paleomagnetic data from whole-core and discrete samples were integrated with biostratigraphic data. Although the biostratigraphic data are poor in many places, reasonable correlations to the geomagnetic polarity time scale back to the middle Miocene were performed on cores from Holes 783A, 784A, and 786A. The data from Hole 782A enabled us to extend these correlations back to the late Oligocene.

Although some correlations were attempted in the older sequences, the poor recovery, complex magnetizations, and sparse biostratigraphic control make these correlations much more tentative.

REFERENCES

- Barron, J. A., 1985. Miocene to Holocene planktonic diatoms. In Bolli, H. M., Saunders, J. B., and Perch-Nielsen, K. (Eds.), *Plankton Stratigraphy*: Cambridge (Cambridge Univ. Press), 763–809.
- Berggren, W. A., Kent, D. V., Flynn, J. J., and Van Couvering, J. A., 1985. Cenozoic geochronology. *Geol. Soc. Am. Bull.*, 96:1407–1418.
- Fryer, P., Pearce, J. A., Stokking, L. B., et al., 1990. *Proc. ODP, Init. Repts.*, 125: College Station, TX (Ocean Drilling Program).

Date of initial receipt: 1 October 1990

Date of acceptance: 6 May 1991

Ms 125B-155

APPENDIX A

WCC Magnetometer Polarity Data for Leg 125

The interpretations are based on the changes in remanence between the natural remanent magnetization direction and direction after demagnetization to 10 mT of the archive cores. Many of the defined polarity intervals are based on the "trend" toward a particular polarity state (N, normal; R, reversed; ?, indeterminate). From these data it is possible to make a polarity evaluation based on the relative shift in direction toward a particular polarity state. Generally, this shift is greatest for levels with a reversed polarity depositional remanence because the antiparallel normal polarity viscous remanent magnetization (VRM) is removed during the early stages of demagnetization (5 to 10 mT). Normal polarity intervals characteristically exhibit smaller changes in direction (less than 10°, as the VRM is aligned subparallel to the detrital remanent magnetization), but up to a 50% decrease in intensity. The position of several thin (10–20 cm) "anomalous" levels is indicated in the "Comments" column.

Core	Polarity	Depth (mbsf)		Comments
		Upper	Lower	
125-782A-				
IH	N	0.0	7.70	
	R		8.10	
	N		9.80	Section 4 not measured at 10 mT
				Two low-inclination swings at 13.00 and 13.90 mbsf
2H	N	9.80	17.25	
	?		18.80	No section
3H	N	19.30	24.80	Notable declination/inclination swing at 25.70 mbsf
	R		28.80	
4H	N	29.10	34.60	
	?		35.20	
5H				Mix-up with core depth record
6H	N	47.80	53.50	R at 51.25 mbsf
	R		57.20	
7H	?	57.30	57.80	
	N		59.25	
	N?		60.65	
	N		61.00	
	R		62.75	
	N		62.90	
	R		63.15	
	N		63.65	
	R		64.25	
	N		64.70	
	R		65.00	
	N		65.20	
	R		65.50	
	N		65.85	
	R		66.20	
	N		66.80	
8H	R	66.80	67.35	
	N		68.10	
	R		69.10	
	N		69.50	
	R		70.10	
	N		70.40	
	R		70.50	
	N		70.95	
	R		74.40	
	N		76.30	
9H	R	76.30	77.60	
	?		79.20	
	N		85.20	
	?		86.00	
	N		86.30	
10X				No core
11X	R	95.70	97.90	
	N		99.60	
12X	R	105.30	110.05	
	N		110.30	
13X	R	115.00	115.45	
	N		115.90	
	?		116.20	
	N		117.70	

APPENDIX A (continued).

Core	Polarity	Depth (mbsf)		Comments
		Upper	Lower	
14X	R		120.00	
	R	124.60	126.00	
	N		129.30	
	R		130.60	
15X	N	134.30	136.70	
	R		139.00	
16X	N	143.90	148.05	
17X	R	153.60	160.20	
	N		161.20	
18X	N	163.20	166.00	
19X	N	172.90	177.90	
20X	R	182.50	183.50	
21X	R	192.10	193.60	
	N		198.90	
22X	R	201.80	203.30	
23X	N	211.50	214.40	
	R		216.00	
24X	N		224.60	
25X	R	230.70	235.40	
	N		236.10	
	R		236.35	
	N		239.70	
	?		240.05	
26X	R	240.30	240.50	
	?		241.30	
	R		242.00	
	N		243.30	
	R		244.10	
	N		244.30	
	R		244.50	
27X	N		253.70	
28X	R	259.60	261.80	
	N		263.75	
	R		264.40	
	N		264.75	
	R		265.30	
	N		266.10	
	R		267.00	
	N		267.25	
	R		268.60	
29X	R	269.20	272.40	
	N		276.70	
	R		278.50	
30X	N	278.80	281.30	
	R		281.45	
	N		281.55	
	R		281.85	
	N		282.10	
31X	R	289.00	289.35	
	N		290.50	
	?		291.40	
32X	?	294.00	297.55	No WCC magnetometer data
	N		300.10	
33X	N	303.50	308.70	
	R		311.10	
	N		313.00	
34X	N	313.10	315.00	
35X	N	322.50	323.35	
	R		324.15	
	N		324.40	
	R		325.10	
	N		327.30	
	R		327.90	
	N		328.10	
	R		328.90	
	N		331.50	
	R		332.00	
36X	N	332.10	335.50	
	R		335.90	
	N		336.40	
	R		336.85	
	N		337.15	
	R		338.70	Plus two N trends at 337.75 and 338.2 mbsf
	N		338.85	
	R		339.20	N at 339.4 mbsf

APPENDIX A (continued).

		Depth (mbsf)		
Core	Polarity	Upper	Lower	Comments
37X	N	341.60	345.50	R at 344.8 mbsf
	R		347.35	N at 346.3 and 346.7 mbsf
	N		349.80	R at 349.35 mbsf
	R		351.00	N at 350.35 and 351.10 mbsf
38X	?			Core too short
39X	?			N-R-N at about 363 mbsf
40X	N	370.50	374.20	
	?		374.40	
	R		374.50	
	N		376.00	
	?		376.25	
	N		376.50	
41X	N	380.20	382.70	
	R		382.90	
	N		384.90	
	R		385.10	
	N		387.20	R at 386.20 mbsf
	R		387.75	
	N		388.35	
	R		388.55	
42X	N	390.00	390.00	R at 389.45 mbsf
	N		392.10	R at 390.10 mbsf
	R		392.40	
	N		392.80	
	R		393.10	
	N		393.25	

125-783A-

1R	N	0.00	1.50	
	R		1.60	
	N		2.50	
	?		3.70	
	N		5.20	
	?		6.20	
	N		7.20	
	?		7.50	
	N		9.00	R trend at 8.6 mbsf
2R	R	9.70	12.00	Good trends toward R
3R				No core
4R	R	26.00	32.50	Good trends toward R
5R	R	35.70	40.70	
6R				No core
7R	R	52.40	56.80	
8R	N	62.10	66.30	R at 65.1 mbsf

125-784A-

1R			No core
2R			No core
3R	N	10.90	11.05
	R		11.35
	N		12.10
	?		12.40
	N		14.70
	R		15.30
	N		15.90
4R	N	20.40	20.80
	R		21.10
	N		21.30
	R		21.80
	N		22.40
	R		25.60
5R			No core
6R	R	39.60	42.75
	N		43.70
			44.10
	N		45.10
	R		45.25
	N		45.60
	R		45.75
	N		47.00
	R		47.60
7R	R	51.00	53.65
8R	R	58.80	59.50
	N		61.60

APPENDIX A (continued).

Core	Polarity	Depth (mbsf)		Comments
		Upper	Lower	
	R		66.50	
9R	R	68.50	75.20	
10R	N	78.10	83.90	
11R				No core
12R	R	97.40	100.20	
13R	R	106.50	107.50	Very short core: only 5 measurements N at 119.70 mbsf
14R	R	116.70	123.70	
15R	R	126.40	136.00	
16R	N	136.00	145.40	? at 142.3, 143.6, and 144.5 mbsf
17R	R	145.70	149.45	
	N		152.20	
	R		153.00	
18R	R	155.40	156.50	
	N		152.20	
	R		165.00	Subhorizontal bedding at 163.93 mbsf
19R	N	165.60	168.30	
	?		168.50	
20R	R	174.40	175.75	
	N		182.10	R at 176.75 mbsf
125-786A-				
1H	N	0.0	0.35	
	R		2.20	
	N		2.50	
	R		4.65	
	N		9.00	
	R		9.30	
2H	N	9.7	11.35	
	R		13.15	
	N		15.40	
	R		17.60	
	N		19.15	
3H	R	19.20	20.75	
	?		22.20	No data
	N		23.60	
	R		25.30	
	N		26.60	
	R		28.70	
4X	N	28.70	30.40	
	R		30.85	
5X	N	38.20	42.65	R at 41.30 and 42.00 mbsf
6X	N	47.60	53.20	
	R		53.50	Cores 5X, 6X, and 7X have good trend behavior
	N		53.95	

No 10-mT WCC data from this section

APPENDIX A (continued).

Core	Polarity	Depth (mbsf)		Comments
		Upper	Lower	
	N		101.80	
	?		102.70	
	N		103.80	
	?		104.00	
	N		104.20	
	?		104.40	

APPENDIX B
DSF Magnetometer Remanence Data for Leg 125 Samples

Core, section, interval (cm)	Depth (mbsf)	Natural remanent magnetization			Remagnetization at 40 mT			Polarity ^a
		Declination (degrees)	Inclination (degrees)	Intensity (mA/m)	Declination (degrees)	Inclination (degrees)	Intensity (mA/m)	
125-782A-								
1H-1, 52	0.52	332.4	55.1	57.1	325.3	70.7	19.1	N
1H-2, 52	2.02	352.2	57.0	84.2	345.7	47.9	21.1	N
1H-3, 52	3.52	349.8	61.2	109.3	340.7	65.5	28.8	N
1H-4, 52	5.02	0.4	55.1	28.9	339.8	46.0	2.7	N
1H-5, 52	6.52	56.7	76.1	54.4	250.0	77.3	5.0	N
1H-6, 52	8.02	107.5	13.8	33.3	137.2	13.7	9.1	?
1H-7, 52	9.52	103.1	37.3	57.6	121.7	40.1	14.7	N
2H-1, 16	9.96	231.1	36.1	30.8	259.4	28.1	20.0	N
2H-2, 16	11.46	296.6	-46.2	2.6	276.1	-26.7	1.1	R
2H-3, 16	12.96	206.5	65.7	14.3	258.5	72.2	4.1	N
2H-4, 16	14.46	253.1	58.7	28.5	243.4	53.8	6.5	N
2H-5, 16	15.96	261.0	62.4	36.4	264.8	48.4	7.6	N
2H-6, 16	17.46	233.6	58.7	80.7	228.3	58.3	19.3	N
2H-7, 16	18.96	251.5	46.8	104.7	255.6	45.7	18.7	N
3H-1, 16	19.46	17.5	70.0	8.0	251.5	-22.8	2.3	R
3H-2, 16	20.96	160.2	53.2	10.2	186.6	57.9	0.7	N
3H-3, 16	22.46	208.4	41.8	18.8	174.6	10.5	3.8	?
3H-4, 16	23.96	208.7	52.1	99.5	215.2	52.2	26.9	N
3H-5, 16	25.46	252.4	-4.8	7.2	42.0	-49.7	4.0	R
3H-6, 16	26.96	39.4	-35.1	44.0	51.4	-45.0	13.8	R
3H-7, 16	28.46	31.4	-44.6	31.3	57.0	-61.5	9.6	R
4H-1, 19	28.99	240.7	33.9	7.6	240.1	23.0	1.0	N
4H-2, 19	30.49	215.2	-1.2	13.2	240.6	20.5	0.8	N
4H-3, 115	32.95	38.2	45.2	13.9	37.2	33.4	2.5	N
4H-4, 19	33.49	209.0	16.1	17.4	205.9	14.2	1.8	?
4H-5, 19	34.99	248.2	-10.0	13.5	239.5	10.7	1.4	?
4H-6, 19	36.49	206.3	-36.6	26.5	234.7	-41.0	9.3	R
4H-7, 19	37.99	227.7	-52.1	26.4	235.9	-59.4	7.1	R
5H-1, 37	38.68	264.6	20.0	5.6	220.0	-37.7	2.2	R
5H-2, 37	40.18	153.8	-9.5	14.6	150.0	-40.0	2.4	R
5H-3, 37	41.68	193.0	-36.8	23.3	188.1	-37.5	7.2	R
5H-4, 37	43.18	219.2	-8.8	5.9	172.1	-15.4	3.8	R
5H-5, 37	44.68	276.7	-26.9	11.0	234.8	-47.7	3.3	R
5H-6, 37	46.18	219.1	-37.4	54.6	209.6	-37.8	12.9	R
5H-7, 16	47.46	219.1	-39.8	35.6	194.9	-44.0	10.5	R
6H-1, 106	48.86	161.5	61.3	10.6	165.0	58.6	2.8	N
6H-2, 23	49.53	193.1	80.4	9.4	169.0	61.0	3.6	N
6H-3, 102	51.82	194.0	42.6	75.0	194.4	43.6	16.3	N
6H-4, 60	52.90	212.5	56.3	99.0	203.0	60.8	25.3	N
6H-5, 64	54.44	357.3	-36.7	32.1	29.0	-54.0	23.9	R
6H-6, 69	55.99	321.9	-73.3	37.3	12.5	-47.0	15.7	R
6H-7, 45	57.25	6.8	-49.1	8.2	11.9	-78.4	3.0	R
7H-1, 44	57.74	319.0	-38.9	19.1	337.0	-27.7	4.0	R
7H-2, 44	59.24	284.5	-65.6	7.8	350.0	-64.5	1.3	R
7H-3, 44	60.74	267.0	-58.9	6.9	44.4	-68.8	2.3	R
7H-4, 44	62.24	185.8	-76.6	7.8	97.6	-45.0	3.4	R
7H-5, 44	63.74	49.4	-31.6	43.1	59.9	-30.8	16.1	R
7H-6, 44	65.24	253.5	16.7	50.9	209.6	-50.8	6.4	R
7H-7, 44	66.74	215.1	-74.5	19.0	130.2	-66.6	6.2	R
8H-1, 27	67.07	247.5	38.5	44.9	347.4	50.3	3.0	N
8H-2, 27	68.57	126.5	-4.3	17.4	206.4	17.0	1.9	?
8H-3, 27	70.07	353.6	23.0	36.9	38.9	15.5	4.3	?
8H-4, 27	71.57	250.8	18.8	20.4	137.6	-55.6	3.8	R
8H-5, 27	73.07	70.0	-46.8	29.9	112.4	-56.3	10.4	R
8H-6, 27	74.57	233.8	74.0	36.7	224.0	61.4	10.1	N
8H-7, 27	76.07	42.6	-28.5	29.3	186.0	44.8	4.0	N
9H-1, 20	76.50	336.2	37.3	30.5	341.0	34.7	8.6	N
9H-2, 20	78.00	328.8	65.8	39.0	353.8	48.6	8.5	N
9H-3, 8	79.38	303.4	39.7	25.4	319.0	32.0	6.3	N
9H-4, 8	80.88	297.9	61.1	35.8	303.8	63.3	7.7	N
9H-5, 8	82.38	144.3	73.3	21.0	31.1	45.1	9.2	N
9H-6, 8	83.88	46.7	60.8	46.7	214.1	-16.9	2.7	?
11X-1, 24	95.94	236.1	-55.6	96.0	274.9	-26.4	13.3	R
11X-2, 24	97.44	111.2	-66.1	96.2	111.5	-58.4	18.1	R
11X-3, 12	98.82	104.8	11.8	68.8	106.3	31.5	18.0	R
12X-1, 60	105.90	13.3	-70.7	36.0	342.6	-72.7	9.9	R
12X-2, 53	107.33	90.3	-47.0	50.1	96.2	-47.2	16.5	R
12X-3, 52	108.83	140.0	-68.8	68.9	154.1	-71.9	22.7	R
13X-1, 109	116.09	73.6	-30.3	8.3	61.4	-3.4	1.2	?
13X-2, 19	116.69	330.1	-77.9	17.9	209.2	-28.7	1.5	R
13X-2, 65	117.05	307.1	38.7	62.2	313.7	46.6	19.9	N

APPENDIX B (continued).

Core, section, interval (cm)	Depth (mbsf)	Natural remanent magnetization			Remagnetization at 40 mT			Polarity ^a
		Declination (degrees)	Inclination (degrees)	Intensity (mA/m)	Declination (degrees)	Inclination (degrees)	Intensity (mA/m)	
13X-3, 81	118.81	14.1	-34.0	39.5	6.1	-31.2	7.5	R
13X-4, 9	119.59	41.5	-46.4	22.6	49.7	-43.4	3.8	R
14X-1, 28	124.88	216.3	-61.8	39.8	215.3	-62.7	11.3	R
14X-2, 28	126.38	207.0	51.6	28.4	214.8	47.2	10.3	N
14X-3, 28	127.88	207.5	44.2	40.8	187.4	43.2	17.6	N
14X-4, 28	129.38	135.5	-43.8	30.6	138.3	-45.8	7.0	R
15X-1, 21	134.51	332.5	-29.5	24.7	287.2	41.7	10.2	N
15X-2, 21	136.01	320.6	24.1	53.9	306.3	54.0	22.0	N
15X-3, 21	137.51	45.7	-69.3	60.2	144.0	-52.7	16.1	R
16X-1, 22	144.12	264.5	27.3	37.0	268.1	32.6	12.0	N
16X-2, 22	145.62	143.1	33.6	80.0	125.3	49.7	27.2	N
16X-3, 22	147.12	273.9	39.5	43.3	288.2	49.4	12.9	N
17X-1, 46	154.06	134.1	-28.1	23.1	262.3	-35.5	2.4	R
17X-2, 46	155.56	136.5	-42.4	39.3	161.5	-41.0	9.0	R
17X-3, 46	157.06	348.0	-46.0	26.3	13.3	-53.0	4.9	R
17X-4, 46	158.56	12.8	-62.7	43.7	341.4	-62.6	11.3	R
17X-5, 46	160.06	83.7	-69.7	24.6	62.0	-65.0	4.8	R
18X-1, 60	163.80	339.9	8.7	18.9	335.8	46.7	8.6	N
18X-2, 60	165.30	44.5	-55.3	71.5	150.9	58.4	15.4	N
19X-1, 80	173.70	219.7	12.3	29.3	225.6	32.3	11.4	N
19X-2, 80	175.20	276.2	37.6	39.4	266.4	44.0	13.7	N
19X-3, 80	176.70	132.0	45.3	34.8	137.8	55.4	11.0	N
19X-4, 22	177.62	19.1	50.3	8.8	320.6	65.3	5.4	N
20X-1, 55	183.05	78.8	-20.1	45.5	145.2	-45.2	22.6	R
21X-1, 103	193.13	359.2	-55.2	102.2	340.9	-43.2	22.5	R
21X-2, 103	194.63	121.6	-73.5	61.4	191.6	-55.1	15.3	R
21X-3, 103	196.13	186.7	41.7	71.4	184.1	49.0	25.5	N
21X-4, 103	197.63	68.8	3.0	34.3	74.7	49.7	12.6	N
21X-5, 83	198.93	347.2	-9.6	70.4	331.6	41.7	19.3	N
22X-1, 55	202.60	248.6	-74.2	33.1	209.4	-63.4	11.0	R
22X-2, 33	203.98	38.7	-30.1	29.5	35.4	-36.2	9.7	R
23X-1, 91	212.41	112.2	42.4	28.9	104.1	47.6	13.4	N
23X-2, 61	213.61	11.2	36.6	143.0	1.0	47.4	44.1	N
23X-3, 82	215.32	47.3	-51.3	17.7	38.5	-38.0	4.5	R
23X-4, 68	216.68	216.6	41.3	33.3	226.4	50.1	8.5	N
23X-5, 58	218.08	64.3	14.0	72.0	84.0	32.5	13.5	N
23X-6, 72	219.72	11.1	-60.2	33.3	234.6	32.0	10.5	N
23X-7, 7	220.57	69.7	82.0	110.5	253.0	54.7	16.9	N
24X-1, 96	221.96	277.8	61.5	76.5	267.8	58.0	22.4	N
24X-2, 106	223.56	159.9	48.2	51.9	182.0	49.4	19.5	N
25X-1, 96	231.66	319.9	-58.0	45.8	326.5	-51.7	15.0	R
25X-2, 60	232.80	129.9	-76.6	27.9	121.3	-75.1	10.1	R
25X-3, 80	234.50	73.1	-55.0	34.0	79.9	-47.5	8.6	R
25X-4, 95	236.15	320.0	-24.6	31.1	151.4	54.0	1.6	?
25X-5, 56	237.26	149.7	44.5	38.3	156.6	68.3	9.2	N
25X-6, 59	238.79	333.9	37.1	45.1	325.8	44.8	14.4	N
26X-1, 9	240.39	127.5	-65.7	40.5	127.2	-47.2	7.7	R
26X-2, 73	242.53	319.3	31.3	27.0	295.7	27.8	8.8	N
26X-3, 126	244.56	35.2	-5.8	7.0	189.4	64.3	0.4	?
26X-4, 107	245.87	140.3	57.5	30.9	303.4	71.0	6.8	N
26X-5, 118	247.48	121.1	37.0	59.4	115.4	43.0	12.7	N
26X-6, 127	249.07	279.6	31.8	12.9	263.5	60.2	5.8	N
27X-1, 117	251.17	110.6	-53.8	76.7	49.8	46.4	7.3	N
27X-2, 134	252.84	272.4	-3.9	45.5	260.4	13.3	11.6	N
27X-3, 56	253.56	4.5	-21.8	25.8	342.9	-2.7	5.6	?
28X-1, 59	260.19	354.8	-57.7	45.6	16.1	-58.7	10.7	R
28X-2, 24	261.34	78.4	-13.0	86.1	56.0	-17.0	23.1	R
28X-3, 49	263.09	258.2	47.1	138.4	262.9	52.2	39.0	N
28X-4, 37	274.63	136.0	-38.0	22.3	56.3	-23.8	4.4	R
28X-6, 105	268.15	348.7	-54.6	31.1	351.0	-63.0	11.0	R
29X-1, 16	269.36	85.9	-57.3	96.1	108.9	-59.4	12.9	R
29X-2, 28	270.98	106.7	-68.8	46.6	220.7	-56.2	11.0	R
29X-3, 7	272.27	104.2	-78.3	24.9	140.6	-63.2	7.2	R
29X-4, 93	274.63	270.0	25.9	39.0	286.4	56.3	16.9	N
29X-5, 9	275.29	101.1	21.1	75.3	88.8	33.3	14.2	N
29X-6, 78	277.48	302.6	-76.7	60.4	259.3	-45.7	27.1	R
30X-1, 41	279.21	188.7	23.1	159.5	180.3	-47.5	60.6	R
30X-1, 61	279.41	159.4	18.3	163.1	180.5	43.8	52.5	N
30X-2, 61	280.36	342.1	-6.4	93.2	308.2	17.0	10.1	N
30X-CC, 6	282.06	15.7	-23.7	77.1	193.2	-77.5	8.1	R
31X-2, 112	290.10	87.4	-34.1	19.3	98.0	18.4	4.2	N
31X-3, 46	290.94	72.0	-53.6	56.8	98.0	-50.2	17.5	R
32X-1, 132	295.32	115.5	-59.2	106.6	136.3	-53.2	46.7	R
32X-2, 90	296.40	29.6	-24.4	19.6	240.7	-45.9	9.2	R
32X-4, 37	298.87	329.2	33.6	194.5	331.4	40.7	54.0	N

APPENDIX B (continued).

Core, section, interval (cm)	Depth (mbfs)	Natural remanent magnetization			Remagnetization at 40 mT			
		Declination (degrees)	Inclination (degrees)	Intensity (mA/m)	Declination (degrees)	Inclination (degrees)	Intensity (mA/m)	Polarity ^a
32X-5, 65	300.65	3.6	-55.6	36.2	254.8	-40.7	14.0	R
32X-6, 56	302.06	119.1	-58.9	90.0	79.8	-64.2	34.3	R
33X-1, 57	304.07	300.4	73.5	156.3	168.6	53.9	24.3	N
33X-2, 13	305.13	220.7	37.5	146.4	223.7	29.9	46.1	N
33X-3, 53	307.03	17.1	59.1	145.3	235.3	28.7	21.7	N
33X-4, 52	308.52	315.7	16.9	83.8	315.3	9.0	16.8	?
33X-5, 53	310.03	199.1	-73.0	54.1	218.3	-72.0	41.4	R
33X-6, 37	311.37	262.9	4.3	87.0	232.5	18.8	9.4	N
34X-1, 62	313.72	12.0	19.5	164.4	351.0	6.6	9.6	?
35X-1, 92	323.42	9.8	-15.4	136.5	3.2	-65.3	18.2	R
35X-2, 42	324.42	168.5	-37.7	8.6	103.5	-43.5	4.6	R
35X-3, 38	325.88	124.6	37.1	398.5	37.1	44.7	9.2	?
35X-4, 44	327.44	81.5	-30.2	30.8	49.1	-51.2	16.7	R
35X-5, 93	329.43	193.9	57.9	79.9	278.2	33.5	4.4	N
35X-6, 75	330.75	20.2	47.6	53.4	97.3	89.1	53.7	?
36X-1, 111	333.21	95.7	50.6	225.3	51.3	27.4	16.8	N
36X-2, 111	334.71	89.8	17.7	103.3	131.8	37.1	26.4	N
36X-3, 128	336.38	358.6	-73.9	46.2	195.0	-53.3	12.8	R
36X-4, 113	337.73	270.5	-21.0	41.6	249.4	-40.9	17.9	R
36X-5, 22	338.32	45.6	-52.3	57.9	53.6	-43.1	15.4	R
37X-1, 50	342.10	214.7	53.9	90.6	232.3	48.3	24.5	N
37X-2, 93	344.03	357.6	53.2	145.9	17.3	46.9	32.1	N
37X-3, 18	344.78	353.9	0.1	190.2	179.5	-52.8	11.9	R
37X-4, 16	346.26	1.5	-35.8	66.8	303.2	-57.0	34.1	R
37X-5, 26	347.86	64.8	30.4	93.8	89.2	-15.0	7.8	R
37X-6, 92	350.02	290.1	3.3	26.5	158.5	-36.5	13.9	R
39X-1, 133	363.01	334.4	6.5	59.6	258.6	-36.5	13.9	R
39X-CC, 10	363.28	316.0	-53.7	42.6	359.4	-4.8	6.8	?
40X-3, 52	374.02	243.7	-0.4	44.3	183.0	-52.3	5.7	R
40X-4, 59	375.59	349.3	32.4	56.9	313.1	26.9	10.9	?
41X-1, 64	380.84	92.7	18.1	133.1	115.3	-0.3	0.9	?
41X-2, 24	381.94	186.5	-11.3	135.8	179.4	34.9	12.2	N
41X-3, 47	383.67	98.2	-32.2	55.8	17.4	-76.9	5.8	R
41X-6, 41	388.11	84.0	21.6	83.3	40.0	-54.5	6.0	R
41X-7, 11	389.31	234.1	36.1	9.8	254.9	19.9	2.6	N
41X-CC, 5	389.60	316.9	-21.6	11.3	304.1	-35.8	3.0	R
42X-1, 58	390.38	42.6	40.0	15.3	330.0	-31.5	1.6	?
42X-2, 107	392.37	53.7	45.8	19.9	335.2	31.1	2.0	?

125-783A-

1R-1, 103	1.03	325.4	30.0	77.3	347.6	53.7	17.6	N
1R-2, 33	1.83	0.5	15.5	71.4	19.0	26.2	24.6	N
1R-3, 6	3.06	343.0	60.2	63.6	330.2	64.0	10.5	N
1R-4, 11	4.61	63.0	74.7	101.0	82.5	62.9	16.2	N
1R-5, 86	6.86	302.4	62.3	90.7	293.4	62.8	20.5	N
1R-6, 89	8.39	344.5	47.8	73.3	340.1	50.6	17.0	N
1R-7, 45	9.45	333.0	74.0	7.6	269.7	13.9	1.9	?
2R-1, 52	10.22	24.7	-54.2	32.7	350.7	-57.1	13.0	R
2R-2, 3	11.23	252.1	-55.0	44.2	253.4	-54.4	12.2	R
4R-1, 114	27.14	33.0	-48.0	25.7	35.2	-74.2	7.2	R
4R-2, 113	28.63	227.7	28.5	14.6	86.7	-28.6	0.8	R
4R-3, 113	30.13	220.2	-32.5	23.1	210.6	-32.7	6.3	R
4R-4, 113	31.63	238.6	-79.1	34.5	97.1	-29.4	16.1	R
4R-5, 40	32.40	92.0	-19.0	62.2	230.8	-77.4	11.9	R
5R-1, 26	35.96	171.4	-82.9	47.3	87.0	-61.6	10.0	R
5R-2, 26	37.46	190.9	-75.8	60.5	188.9	-67.2	23.4	R
5R-3, 26	38.96	87.1	-51.7	99.2	106.4	-52.5	28.4	R
5R-4, 13	40.33	262.2	-50.7	67.1	283.2	-51.9	11.6	R
7R-1, 90	53.30	122.7	-67.7	68.9	111.2	-56.2	18.1	R
7R-2, 90	54.80	110.5	-53.6	82.5	118.3	-71.2	21.1	R
7R-3, 90	56.30	182.1	-64.3	84.6	193.3	-65.2	21.8	R
7R-4, 3	56.93	339.0	-46.2	118.0	335.4	-49.7	27.9	R
8R-1, 120	63.30	262.8	53.7	123.0	268.6	53.4	35.4	N
8R-2, 120	64.80	86.5	55.3	48.7	99.3	56.1	13.6	N
8R-3, 91	66.01	278.8	44.5	41.6	303.3	27.0	13.8	N

125-784A-

1R-1, 68	0.68	225.8	-50.1	50.5	237.6	-45.1	7.9	R
1R-CC, 17	1.11	279.3	42.2	63.3	274.3	48.2	12.4	N
3R-1, 85	11.75	150.5	40.1	37.9	126.6	42.8	9.4	N
3R-2, 85	13.25	79.2	45.3	86.0	65.4	35.7	17.3	N
3R-3, 85	14.75	67.7	42.6	124.2	41.9	61.7	25.4	N
3R-4, 85	15.65	202.5	45.3	150.6	205.0	44.2	27.5	N

APPENDIX B (continued).

Core, section, interval (cm)	Depth (mbsf)	Natural remanent magnetization			Remagnetization at 40 mT			Polarity ^a
		Declination (degrees)	Inclination (degrees)	Intensity (mA/m)	Declination (degrees)	Inclination (degrees)	Intensity (mA/m)	
4R-1, 60	21.00	309.6	13.0	38.2	15.4	-23.8	25.6	^b R
4R-2, 97	22.87	312.6	-37.4	57.2	314.1	-45.7	21.1	R
4R-3, 97	24.37	51.9	-33.7	54.4	53.9	-40.6	18.8	R
4R-4, 59	25.49	160.0	30.9	42.3	157.6	36.6	5.7	N
6R-1, 60	40.10	306.5	-55.6	67.5	310.2	-59.3	19.0	R
6R-2, 57	41.57	162.4	-48.1	119.1	155.2	-34.7	21.7	R
6R-3, 52	43.02	215.8	31.4	38.9	218.2	39.0	11.2	N
6R-4, 69	44.69	7.5	52.1	65.8	9.9	53.4	19.2	N
6R-5, 51	46.01	196.7	-15.6	19.1	192.4	-28.1	7.1	R
6R-6, 58	47.58	344.3	-23.2	25.0	331.8	-19.8	9.8	R
7R-1, 39	49.49	26.3	-23.5	30.3	25.9	-22.4	20.9	R
7R-2, 109	51.69	350.0	-12.3	51.2	342.4	-23.9	15.7	R
7R-3, 112	53.22	206.4	-25.8	44.7	215.4	-32.4	11.5	R
8R-1, 82	59.62	278.7	27.8	18.8	294.5	29.8	5.1	N
8R-2, 82	61.12	185.4	6.6	33.1	180.4	-3.4	8.3	R
8R-3, 82	62.62	63.7	-40.8	145.8	59.3	-41.0	37.6	R
8R-4, 82	64.12	261.3	-23.9	109.2	268.5	-27.9	30.2	R
8R-5, 82	65.62	34.6	-13.2	61.3	26.8	-26.8	15.2	R
8R-6, 8	66.38	217.5	-31.9	95.6	224.1	-39.0	29.1	R
9R-1, 14	68.64	328.9	-22.4	44.0	326.2	-22.3	14.0	R
9R-2, 14	70.14	341.9	-59.8	190.2	340.0	-54.1	51.6	R
9R-3, 14	71.64	59.7	-38.7	83.0	68.3	-34.8	18.5	R
9R-4, 14	73.14	279.2	-33.9	90.0	256.9	-25.7	30.5	R
9R-5, 14	74.64	177.6	-25.3	80.2	155.6	-51.0	16.8	R
10R-1, 53	78.63	295.1	50.3	40.0	284.3	45.9	7.9	N
10R-2, 30	79.90	122.2	44.6	54.2	113.9	40.8	13.7	N
10R-3, 83	81.93	19.8	45.7	114.2	21.2	47.0	39.2	N
10R-4, 13	82.73	47.6	40.6	122.5	54.0	39.1	33.7	N
12R-1, 12	98.61	110.9	-3.8	161.4	103.9	-8.1	47.4	R
12R-2, 58	99.48	268.9	-18.6	99.3	270.2	-22.7	31.3	R
13R-1, 28	107.38	52.2	3.2	26.2	42.3	-37.0	25.9	R
14R-1, 108	117.78	211.8	-7.4	110.2	212.7	-18.2	31.6	R
14R-2, 74	118.94	344.2	-3.9	113.2	43.4	1.9	38.3	?
14R-3, 83	120.53	66.3	-27.3	142.1	68.2	-29.5	43.2	R
14R-4, 21	121.43	198.0	-21.2	76.1	214.9	-41.0	20.3	R
14R-5, 36	123.06	131.6	-23.8	142.4	128.3	-28.7	40.0	R
15R-1, 123	127.63	281.3	-16.8	121.2	79.5	-18.1	33.4	R
15R-2, 123	129.13	239.3	-31.3	161.1	243.8	-34.6	46.4	R
15R-3, 122	130.63	95.5	-23.5	128.7	101.6	-26.9	35.0	R
15R-4, 122	132.13	343.3	-30.1	105.3	343.1	-32.8	26.2	R
15R-5, 122	133.63	125.2	-34.8	170.7	124.1	-39.1	51.9	R
15R-6, 122	135.13	261.1	-27.0	59.4	280.7	-33.3	18.4	R
15R-7, 34	135.74	273.1	-25.9	71.9	273.8	-30.0	21.0	R
16R-1, 109	137.09	286.7	0.3	22.6	280.7	15.7	9.7	N
16R-2, 109	138.59	204.9	13.3	55.1	206.6	15.5	13.8	N
16R-3, 109	140.09	133.7	30.0	109.6	130.9	22.6	27.4	N
16R-4, 109	141.59	210.3	28.3	105.5	284.3	37.9	3.5	N
16R-5, 109	144.59	262.8	31.6	93.9	223.8	26.2	22.9	N
17R-1, 96	146.56	223.0	-8.0	67.3	222.2	-14.2	15.3	R
17R-2, 96	148.06	197.9	-40.1	37.7	220.0	-54.3	10.0	R
17R-3, 96	149.56	188.9	50.1	10.0	201.7	61.7	2.8	N
17R-4, 96	151.06	261.4	52.3	43.7	266.3	23.7	10.3	N
17R-5, 91	152.51	270.7	-34.8	44.5	272.0	-37.4	12.8	R
18R-1, 96	156.26	331.1	-7.6	265.3	327.2	-6.5	70.3	?
18R-2, 96	157.73	209.6	26.5	135.4	219.2	7.8	39.6	?
18R-3, 115	159.45	46.0	54.4	103.4	46.9	50.7	29.5	N
18R-4, 108	160.88	238.7	-87.3	31.2	286.1	-76.2	8.8	R
18R-5, 111	162.41	170.1	-16.0	43.7	160.0	-21.6	10.4	R
18R-6, 113	163.93	81.5	-33.9	44.7	75.7	-45.1	12.8	R
19R-1, 48	165.48	169.7	15.2	83.9	151.8	52.7	13.8	N
20R-1, 115	175.85	262.3	1.5	9.6	218.8	-6.4	3.2	R
20R-2, 86	177.06	325.9	47.2	39.5	330.1	41.4	12.4	N
20R-3, 57	178.27	7.0	4.5	157.3	330.6	26.1	35.1	N
20R-4, 146	180.66	49.9	24.3	40.0	40.3	9.2	9.6	R

125-786A-

1H-1, 39	0.39	157.5	9.8	31.7	156.2	-45.5	8.7	R
1H-2, 39	1.89	231.4	-23.4	271.4	198.0	-52.9	22.5	R
1H-3, 38	3.38	324.2	11.2	193.6	180.0	-48.0	15.2	R
1H-4, 43	4.93	1.0	44.4	64.6	8.2	26.2	19.6	N
1H-5, 43	6.43	345.6	45.3	167.2	13.1	35.1	27.3	N
1H-6, 31	7.86	16.7	34.7	41.9	21.1	13.3	5.9	?
1H-7, 51	9.51	172.8	-20.9	29.7	173.8	-34.5	13.6	R
2H-1, 134	11.04	228.3	-27.3	184.2	223.5	44.8	21.7	N

APPENDIX B (continued).

Core, section, interval (cm)	Depth (mbsf)	Natural remanent magnetization			Remagnetization at 40 mT			Polarity ^a
		Declination (degrees)	Inclination (degrees)	Intensity (mA/m)	Declination (degrees)	Inclination (degrees)	Intensity (mA/m)	
2H-2, 131	12.51	24.8	-46.2	147.9	347.5	-46.3	19.3	R
2H-3, 132	14.02	210.5	7.0	442.0	178.6	34.9	13.0	N
2H-4, 133	15.53	191.5	52.4	17.4	219.3	70.0	3.9	N
2H-5, 137	17.07	12.8	-34.2	30.9	338.0	-52.0	17.5	R
2H-6, 134	18.54	193.9	43.1	67.9	201.7	40.9	19.2	N
2H-7, 53	19.23	198.4	51.8	68.8	200.9	60.6	15.7	N
3H-1, 123	20.43	110.9	-69.9	39.6	198.5	-61.1	16.2	R
3H-2, 123	21.93	251.3	-67.2	22.5	205.6	-33.3	5.8	R
3H-3, 123	23.43	47.4	31.5	36.6	19.4	3.4	2.8	^b R
3H-4, 123	24.93	94.0	-55.5	16.2	196.6	-46.4	6.5	R
3H-5, 123	26.43	39.9	37.0	25.6	9.7	48.3	4.8	N
3H-6, 123	27.93	225.0	-46.5	21.9	227.9	-57.8	12.1	R
3H-7, 36	28.57	248.6	-31.8	35.1	231.5	-46.7	17.7	R
4X-1, 117	29.87	351.1	1.9	8.8	261.4	80.2	1.7	?
5X-1, 120	39.40	22.2	53.2	23.6	21.4	62.0	6.6	N
5X-2, 120	40.90	193.4	0.9	19.5	168.9	22.7	4.4	N
5X-3, 120	42.40	50.9	35.5	43.5	6.9	60.1	9.7	N
5X-4, 72	43.42	194.6	32.6	43.4	229.2	38.0	7.7	N
6X-1, 11	48.75	228.3	44.5	54.2	228.9	36.0	13.4	N
6X-2, 112	50.22	31.3	76.4	63.7	63.7	27.6	16.5	N
6X-3, 112	51.52	37.6	21.2	19.3	321.4	-8.6	2.8	R
6X-4, 112	53.22	38.9	-18.5	35.9	30.0	-46.7	13.0	R

^a N, normal; R, reversed; ?, indeterminate.^b Remanent magnetization at 50 mT.